Fog Detection System Based on Computer Vision Techniques

S. Bronte, L. M. Bergasa, P. F. Alcantarilla
Department of Electronics
University of Alcalá
Alcalá de Henares, Spain
sebastian.bronte, bergasa, pablo.alcantarilla@depeca.uah.es

***Abstract*—In this document, a real-time fog detection system using an on-board low cost b&w camera, for a driving application, is presented. This system is based on two clues: estimation of the visibility distance, which is calculated from the camera projection equations and the blurring due to the fog. Because of the water particles floating in the air, sky light gets diffuse and, focus on the road zone, which is one of the darkest zones on the image. The apparent effect is that some part of the sky introduces in the road. Also in foggy scenes, the border strength is reduced in the upper part of the image. These two sources of information are used to make this system more robust. The final purpose of this system is to develop an automatic vision-based diagnostic system for warning ADAS of possible wrong working conditions. Some experimental results and the conclusions about this work are presented.**

***Index Terms*—Fog detection, visibility distance, computer vision, growing regions.**

I. Introduction

Advanced Driver Assistance Systems (ADAS) have become powerful tools for driving. In fact, applications based on this concept are nowadays widely extended in vehicles, added as extras to make driving more safety and comfortable. Some examples of this kind of applications are parking-aid, automatic cruise control, automatic switching on/off beams, etc.

Computer vision plays an important role in the development of these systems to cut off costs and provide more intelligence. There are some problems to be solved in the ADAS based in computer vision technologies. One of these problems is the fog detection, which depends on different kinds of weather (cloudy, foggy, rainy, sunny, etc) and also illumination environment conditions. Automatic fog detection can be very useful to switch on-off ADAS when fog makes that these systems do not work properly. Also it can complement intelligent vehicle based applications such as the ones described in [1], [2], since a simple output for turning on/off the fog beams, and even thought it can be used for warning the driver to avoid possible collisions when foggy weather conditions are present.

Fog detection is a challenging problem because it depends on unknown information as: depth, weather and lighting conditions. The problem is under-constrined if only an b&w onboard camera is used or real-time computation is needed. Many methods have been proposed in the literature by using multiple images or additional information, without taking into account real-time constraints. Polarization based methods [3], [4] use two or more images taken with different degrees of polarization. In [5], [6], more constraints are obtained from multiple images of the same scene under different weather conditions. Depth based methods [7] require information either from the user inputs or from known 3D models.

Recently, single image fog detection has made significant progresses. The success of these methods lies in using a stronger assumption and they cannot be computed in real-time. Tan [8] observes that the foggy-free image must have higher contrast compared with the input foggy image. The results are visually compelling but may not be physically valid. Fattal [9] estimates the albedo of the scene and then infers the medium transmission, under the assumption that the transmission and surface shading are locally uncorrelated. This approach may be failed in heavy foggy cases, where the assumption is broken. He at al. [10] propose a simple but effective image prior, to detect fog using a fix color camera. It is based on a key observation: most local patches in foggy-free images contain some pixels which have very low intensities in at least one color channel. The dark channel prior may be invalid when the scene object is inherently similar to the airlight over a large local region and no shadow is cast on the object.

Real-time fog detection from a b&w on-board camera has been lightly covered in the literature. Most important works can be found in [11], [12], [13]. In these papers, Hautière et al. showed that based on the effects of Koschmieder's Law [14], light gets diffuse because of the particles of water floating in the air. Using this effect, gray level variation in the horizon is used to measure the amount of fog in the image and then give an estimation of the visibility distance.

Based on the explained idea, we found out someother characteristic effects that are present on the images under fog conditions. In order to robust fog detection the two main characteristics we notice in a foggy image are the decrease of the visibility distance on the image, and the scene blurring due to the loss of high frequency components.

Then, as difference with other works existing in the state of the art, our algorithm has to comply with the following conditions:

- Results have to be accurate, i.e. all foggy situations have to be detected properly, whereas the false alarm probability (i.e. determine fog when the image is not foggy) has to be zero.
- The algorithm has to be fast and able to work under real

time constraints. This is in fact an important constraint for a diagnosis function, since they are going to be integrated into more complex intelligent vehicles systems which consume a lot of computing resources.
- The algorithm has to be able to manage with different day scenarios such as: sunny, cloudy, rainy ...

Section II shows our algorithm proposal. In section III we present some experimental results, conclusions are presented in section IV and finally we comment the future works in section V.

II. Architecture

This section provides general information about the proposed algorithm. First of all, a general task diagram of the implemented algorithm is shown in Fig. 1. Then the most important tasks will be described.

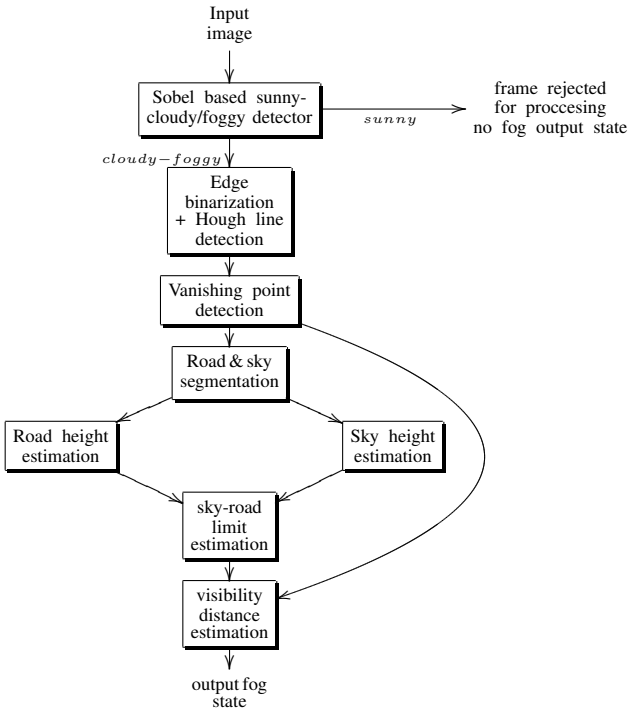

Figure 1: General algorithm description

A. Sobel based sunny - foggy detector

One of the most important effects of fog presence on a image is the reduction of high frequency components, that can be properly measured using edge detection methods, based on Sobel filtering. Foggy images are blurrier and have lower contrast than the sunny ones. It means that information in the higher frequencies is lower in foggy images, rather than in sunny ones. Furthermore, this effect is more significant in the top half of the image.

In order to reduce processing time in the whole algorithm, the original B&W images captured from the micro-camera are resized to 320 x 240 pixels. It is not necessary to have a higher resolution for fog detection.

In typical ADAS applications, where a micro-camera is mounted in the car's windshield area looking up the road, vehicles can be located at different areas of the image. It is more probably to find preceding vehicles in the central area of the image (just in front of the windshield), but also incoming vehicles can be found in lateral areas of the image. Besides, fog effect is not uniformly distributed in the image. For this reason a ROI is defined in the image, and different areas of analysis are considered.

After the ROI is automatically computed in the first frame, Sobel edge detector is used to distinguish between cloudy / foggy and sunny images. We mainly focus on the top half of the filtered image. The more abrupt the edge is, the higher gray level in the output image. Generally, when sunny conditions are present, edge responses are higher than for foggy conditions. Examples of two images with this filtering applied can be shown in Fig. 2, and a comparative figure explaining this subject is shown inside section III.

Edge information does not provide enough resolution to differentiate between moderate fog (about 200 m of visibility distance) and high fog (less than 100 m of visibility distance) states because the difference between these two cases is not straightforward doing a simple edge analysis. An example of these two states is shown in Fig. 8. Therefore the use of visibility distance is necessary to complement this deficiency. Also visibility distance estimation, as it will be shown in Section II-D, can yield to bad results because of the segmentation process in sunny or low fog images.

(a) Sunny input image

(b) Sobel filtered image from the sunny input one

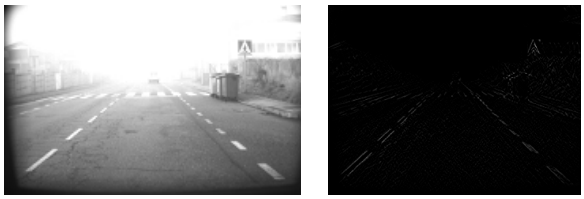

(c) Very foggy input image

(d) Sobel filtered image from foggy the input one

Figure 2: Sobel images in different fog states

B. Vanishing point calculation

If there is some fog in the image, an optimal binarization is applied to the sobel image to enchance the most clear edges. Parameters for this edge detector are fixed in order to have the same reference values for all the sequences. Then, these edge

images are computed with a Hough line detector[15], used to estimate edge lines of the road. Filtering the lines found by the Hough detector to get them enough separated and obtaining its parameters as it was explained before, the vanishing point of the image is found. Fig. 3 depicts the result of this process:

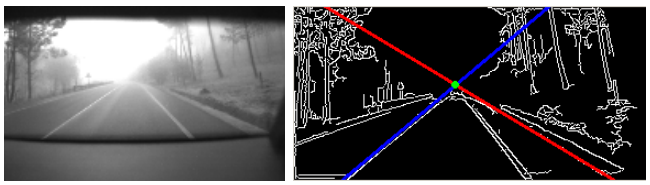

(a) Input image (b) Edge binarized image with filtered lines plotted

Figure 3: Edge filtering, Hough line detection with filtered parameters and vanishing point calculation

The vanishing point of an image is the point where parallel lines which are not perpendicular to the optical axis cross in a image. Road lines are taken as a reference of lines which are parallel and not perpendicular to the optical axis. As a consequence, the vanishing point is easy to find.

Road edge lines founded by the Hough detector were filtered to obtain two good ones to get a good approximation of the vanishing point. Polar coordinates are used in the Hough line detector, therefore a pair (ρ_i, θ_i) is given for each line. To get the Cartesian parameters in order to calculate the vanishing point, the transformation needed is the following:

$$a_i = \cos(\theta_i),\ b_i = \sin(\theta_i) \Longrightarrow \alpha_i = -\frac{a_i}{b_i},\ \beta_i = \frac{\rho}{b_i} \quad (1)$$

On the image, these two filtered lines would have the following equations:

$$v_0 = \alpha_1 u_0 + \beta_1 \quad (2)$$

$$v_0 = \alpha_2 u_0 + \beta_2 \quad (3)$$

where (α_1, β_1) and (α_2, β_2) are the two lines parameters in Cartesian coordinates, converted from polar coordinates, which are obtained from the Hough transform. Solving these last two equations the following one will be obtained:

$$u_0 = \frac{\beta_2 - \beta_1}{\alpha_1 - \alpha_2} \quad (4)$$

and substituting u_0 in one of the two line equations above, the vanishing point height v_0 can be found. An example of this procedure can be seen in Fig. 3.

C. Road and sky segmentation

After the vanishing point is found, a segmentation process is applied using a growing regions approach based on seeds, described in [16], to find the limit between the sky and the road.

Sky is easy to find, if it is present, because most of sky pixels have pure white color, the segmentation process very fast. A single seed point is selected as a random pure-white pixel on the supposed sky area.

To segmentate the road, a seed point is placed in an area where is highly probable to find the road. Some parameters are automatically adapted depending on road's characteristics, for instance, the average value of gray level in a neighborhood of a road pixel. Depending on this average level, the upper difference limit goes up when road gets brighter. This is because the brighter the road is, the greater variation of gray level the pixels in a neighborhood is obtained. Some road image samples from the tested sequences are depicted in Fig. 4 to show the different conditions that the growing regions algorithm has to deal with.

(a) cloudy and low fog road image (b) cloudy and high fog road image (c) sunny road image (with shadows)

Figure 4: Image samples to show the different characteristics of the road

To make the process of finding the sky-road limits easier to the rest of the algorithm, dilate operator is applied in order to full some smal holes in the sky blob. The same process is applied for the road blob. Sky blob is depicted in white color and road blob in black in Fig. 5.

In order to find the limit between the sky and the road, these two segmented images are treated separately. Sky and road image limits are searched from bottom to top, but there are some differences in the procedure. Taking the average of this two limits, the limit between sky and road is found. If the sky is not present, like in some of the test sequences, only the road limit is taken. In the case of the sky image, the most common effect is that the part of the sky over the ground is narrow and the part in the sky is wider. In this case, there is an abrupt transition that can be easily located. On the other hand, considering the road segmented image this abrupt transition is not significant. If the road is well segmented, it is limited by the gray zone in which it is located, but if the scene is very foggy a bad segmentation or an erroneous limit can be obtained. In both cases, if the obtained limit is not logical, i.e. it is above the vanishing point, the vanishing point height will be used as the limit for that frame.

In Fig. 5, some examples of segmented images using the proposed method are shown for the sky 5.b and the road 5.c. When the input image is foggy, a part of the road is segmented as sky in the sky image when this algorithm is used. On one hand, in the sky image, the white part of the image which is the narrowest, is considered the sky limit. On the other hand, in the road image, when no black color is detected, the limit is established.

(a) sky segmented image (b) road segmented image

Figure 5: Segmented foggy images to find road and sky limits

D. Visibility distance measurement

Visibility distance depends on the relative sky-height. This concept means that, when there is some fog in a scene and road is segmented, some part of sky gets into the road part, and the limit between the sky and the road go down. If the image is not foggy, sky and road height on the image are both the same and equals to the vanishing point height, but in a foggy image, apparent sky height is lower than the vanishing point.

This algorithm works with a monocular camera, therefore 3D structure information is not directly available, but an estimation can be made using camera projection equations projection. In general,

$$u = \frac{X - X_0}{Z + f} \tag{5}$$

$$v = \frac{Y - Y_0}{Z + f} \tag{6}$$

The infinite depth distance $(z \to \infty)$ is projected into the vanishing point (u_0, v_0) according to:

$$u_0 = \lim_{z \to \infty} \frac{X - X_0}{Z + f} = 0 \tag{7}$$

$$v_0 = \lim_{z \to \infty} \frac{Y - Y_0}{Z + f} = 0 \tag{8}$$

However, the solution $(0, 0)$ is not a normal point of projection, so the Eq. 5 and 6 have to be rewritten as follows:

$$u - u_0 = \frac{X - X_0}{Z + f} \tag{9}$$

$$v - v_0 = \frac{Y - Y_0}{Z + f} \tag{10}$$

The "Y" axis is selected because fog effect affects the apparent height of the sky on the image, as can be seen in Fig. 5, and X is independent from this effect. By using Eq. 10 Z component can be solved. If a good camera calibration is known, a good depth estimate can be obtained according to the following:

$$Z = f \frac{Y - Y_0}{v - v_0} + f \tag{11}$$

where $Y - Y_0$ and f can be easily obtained from the calibration process, since is the relative height from the ground to the camera and the focus distance respectively; v is be obtained from the relative sky height on the image and v_0 from the height of the vanishing point.

To obtain the depth 'Z' component, we obtain the difference between the vertical coordinate of the limit sky – road, and the vanishing point as it was explained before. With this difference computed and the calibration parameters of the camera, we project this into the 3D world and obtain the depth distance. Calibration parameters were experimentally estimated to obtain reasonable values of visibility distance on the tested sequences.

The estimation in a single frame is very unstable because the limit between sky-road can variate substantially depending on the segmentation results and the camera saturation. In addition, the vanishing point height can also variate due to car vibrations.

Because of that, a filter to alleviate these effects has been implemented. The adopted solution for this problem is to take the median every T seconds. In this period of time, the vanishing point heights and sky-road, limits are registered and the median of each array is calculated when every period is finished. This time is long enough to ease the effects of car's vibrations and fluctuations in the estimated sky-road limit. Another trials have been made, e.g. taking the average instead of the median, or registering samples during a shorter period of time.

Once these two parameters are obtained and Z component is calculated, the specified limits in Table I are used in order to differentiate between the different fog levels. The maximum theoretical visibility distance is about 2 km or above and there is no minimum for visibility distance as it depends on the sky road limit and the calibration parameters. These are based on a common meteorologic criteria to establish the visibility distance.

	upper limit (m)	lower limit (m)
low fog - sunny	-	300
moderate fog	300	100
high fog	100	-

Table I: Visibility distance limits for each fog state

III. Results

In this section the results of the algorithm are shown. Firstly, we show Sobel edge detector results, then some results without and with Sobel edge information will be shown to prove the necessity of the both systems working together, and finally some global statistics about confidence rates of the whole algorithm are described.

Fig. 6 depicts the average level of the Sobel half top images for 4 different sequences. The Sunny sequence has the highest edge level (blue). The Cloudy sequence without fog (green) has high levels, but not as high as the sunny one. As we can see, medium fog (magenta) and high fog (red) can not be

distinguish between them properly with this method but if a good threshold is applied (3 is clearly a good one) sunny – and low foggy levels can be distinguished from medium and high fog states. Because this part of the algorithm can not estimate if it is a high fog or medium fog level, the visibility distance estimation module is implemented.

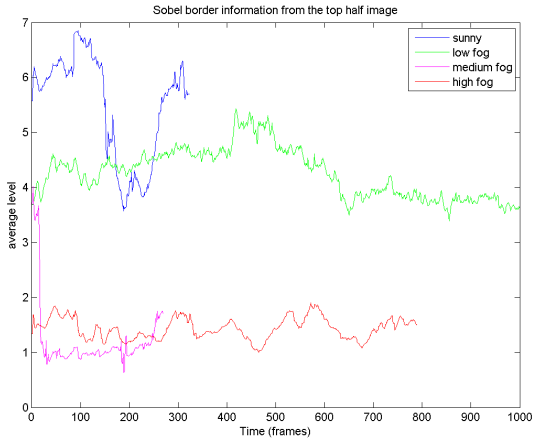

Figure 6: Sobel statistics in various levels of fog

To show the necessity of a complementary system, some estimated visibility distances are shown in Fig. 7a. As it can be observed in Fig. 6 and 7a, colors for each sequence are the same in both images. It can be seen that in the sunny images very low visibility distances are obtained, and in other sequences, normal values for each level are obtained (once they are filtered).

A comparison between the system without correction border compensation and the whole system is shown in Fig. 7a and 7b. In these two figures, the system output are shown. In this figures, during the first period of time, no correct data is available because the vanishing point and the road-sky limit heights are registered to show the first corrected measurement.

This algorithm has been tested with 32 sequences that have different fog levels (cloudy with low, medium and high fog) and also a sunny sequence is included to test if the algorithm works properly in this particular atmospheric condition. The length of the tested sequences are variable and different rates for each one have been obtained. The framerate is 30 fps. The total amount of tested frames is about 36028. Following strictly the given ground truth information, a confidence over 83 % is obtained, but in long sequences, there are some parts in which the atmospheric conditions change, so the ground truth information would also change and over 87 % of confidence is obtained. A summary table containing results of confidence level of the system, ordered by fog level, is shown in Tab. II.

Fig. 8 depicts the final result of processing a high fog and a medium fog sequence. Both the estimated visibility distance and the FOG State variable are shown in the figure. The

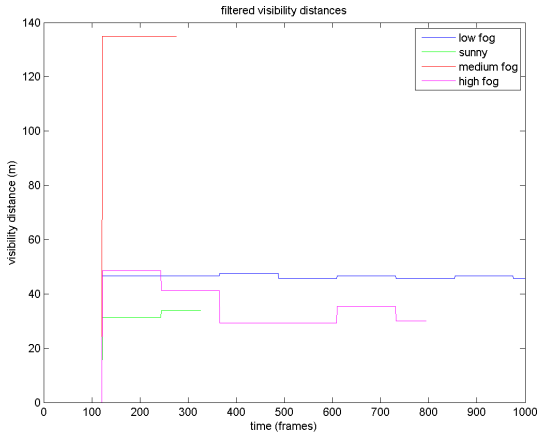

(a) Corrected visibility distance without taking in consideration Sobel edge information

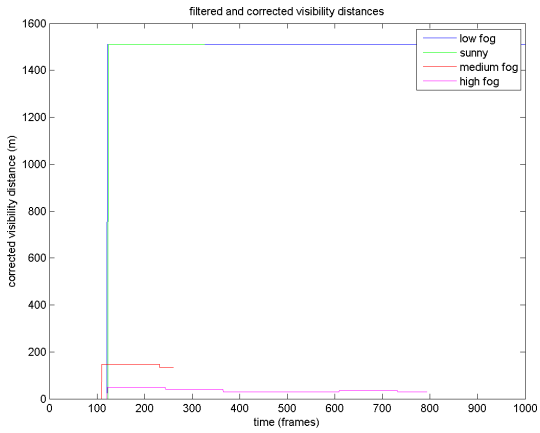

(b) Corrected visibility distance taking in consideration Sobel edge information

Figure 7: Visibility distances for each sample sequence taking and without taking in consideration Sobel edge information

Ground truth	Number of videos	Total length (frames)	Correct estimation rate (%)
low fog and sunny	5	17511	81,3
medium fog	5	2031	88,1
high fog	22	16486	85,3
Total	32	36028	83,5

Table II: Summary of results obtained from the test sequences

horizontal green line shows the vanishing point's height, and the blue one shows the sky-road limit calculated from the sky and road segmented images.

The influence of the used parameters in this software has been studied. In the edge detector, bad threshold values can cause a lose of road lines or the detection of lots of them, and then taking more time to filter them. Morever, Hough line detector parameters are fundamental to do this task faster and taking the most important lines. In calibration parameters, a bad estimation can cause a failure deciding between medium and high fog states. Finally, floodfill parameters are fundamental because a bad segmentation of the road and the sky has effect on the visibility distance estimation, and as a

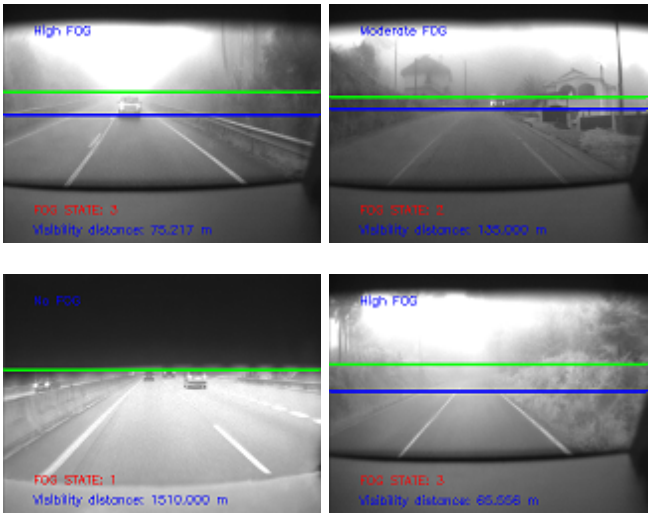

Figure 8: Output sample images for sunny and foggy environments

consequence, a misclasification between fog states.

IV. Conclusions

In this section, final remarks and conclusions for the proposed method are presented:

- The algorithm provides accurate results for fog detection using 3 different levels previously defined in the ground truth (sunny / cloudy with low fog, cloudy with medium fog and cloudy with high fog). The probability of a correct detection is high, over than 85 %. Then, some errors are due to the sample time used for integrating the measurements. If we consider that this kind of signal should be a very low frequency one, about one output measure per minute, its performance would be increased.
- For a better accuracy of the system, a continuous signal about the fog level could be used instead of the 3 levels of the Fog State variable. This signal would be based on the visibility distance and the edge information.
- In some of the tested sequences, the system detects fog when it is really not present, since the visibility distance given by the algorithm is very short. This is because the sun sometimes is very bright and saturates the camera. As a consequence, the segmentation process fails. It can not be considered as a failure, because the sun effect is very similar to the fog one, provoking a short visibility distance that makes very difficult for a normal driving, i.e. on sunrise and sunset.
- The only scenario when this algorithm really fails is when, in a foggy sequence, a long chain of cars appears in the opposite lane of the road (near the horizon line). In this case, the average edge density goes up making the edge level being as similar as the one considering a not foggy scenario instead of a foggy one.
- The algorithm is fast enough to be embedded in a real time system.
- The algorithm can work with different camera configurations and environments, if camera calibration parameters are known or estimated.
- This algorithm is based on edges density and visibility distances, so there can be cases such as a traffic jams, very sunny images or other unexpected artifacts, that can yield an invalid output value.

V. Further work

In a near future, this algorithm will be tested with more sequences in order to prove the real performance with more time and more real situations, and once it work properly in a huge variety of situations, the algorithm will be implemented in a real time system on a real car.

The next step will be the adaptation of the algorithm to night sequences, in order to make the system functional in more ligthing situations.

A weak point was obtained in the algorithm when we were testing the sequences. This problem is not very frequent but it happened in some high foggy sequences. This is due to a long chain of cars appeared in the top half of the images. Because of that, edges density went up, and the algorithm classify the sequence as not foggy level. Some ways to solve this problem will be studied with the new sequences.

VI. Acknowledgments

This work has been supported by the multinational company FICOSA INTERNATIONAL. Then, it has been supported in part by the Spanish Ministry of Science and Innovation under grant TRA2008-03600 (DRIVER-ALERT project). We would like to thank FICOSA-Galicia the collaboration in the recording of the test videos.

References

[1] IEE.Conf.Publ.No.483. Adas. international conference on advanced driver assistance systems. Number 483, 2001.

[2] Rolf Adomat, Georg-Otto Geduld, Michael Schamberger, and Peter Reith. Advanced driver assistance systems for increased comfort an safety - current developments and an outlook to the future on the road. *Advanced Microsystems for Automotive Applications*, 2:431–446, 2003.

[3] S. G. Narasimhan Y. Y. Schechner and S. K. Nayar. Instant dehazing of images using polarization. *CVPR*, (1):325, 2001.

[4] E. Namer S. Shwartz and Y. Y. Schechner. Blined haze separation. *CVPR*, (2):1974–1991, 2006.

[5] S. G. Narasimhan and S. K. Nayar. Chromatic framework for vision in bad weather. *CVPR*, pages 598–605, 2000.

[6] S. G. Narasimhan and S. K. Nayar. Contrast restoration of weather degraded images. *PAMI*, (25):713–724, 2003.

[7] J. Kopf, B. Neubert, B. Chen, M. Cohen, D. Cohen-Or, O. Deussen, M. Uyttendaele, and D. Lischinski. Deep photo: Model-based photograph enhancement and viewing. *SIGGRAPH Asia*, 2008.

[8] R. Tan. Visibility in bad weather from a single image. *CVPR*, 2008.

[9] R. Fattal. Single image dehazing. *SIGGRAPH*, pages 1–9, 2008.

[10] X. Tang K. He, J. Sun. Single image haze removal using dark channel prior. *CVPR*, pages 1956–1963, 2009.

[11] N. Hautière, R. Labayrade, and D. Aubert. Real-time disparity contrast combination for onboard estimation of the visibility distance. *IEEE Transactions on Intelligent Transportation Systems*, 7(2):201–212, 2006.

[12] Nicolas Hautière, Jean-Philippe Tarel, Jean Lavenant, and Didier Aubert. Automatic fog detection and estimation of visibility distance through use of an onboard camera. *Mach. Vis. Appl.*, 17(1):8–20, 2006.

[13] N. Hautière, R. Labayrade, and D. Aubert. Estimation of the visibility distance by stereovision: A generic approach. *IEICE Transactions on information and systems*, 89(7):2084–2091, 2006.

[14] Middleton W.E.K. *Vision Through the Atmosphere*. University of Toronto Press, 1952.

[15] Duda R. and Hart P. Use of the hough transform to detect lines and curves in pictures. *Comm. ACM*, 15(1):11–15, 1972.

[16] R. Adams and L. Vishchof. Seeded region growing. *IEEE Transactions on Pattern Analysis and Machine Intelligence*, 16(6):641–657, 1994.